Highly viscous polymeric foam flowing through an orifice

Ching-Hsien Chen*, Bart Hallmark and John Frank Davidson

Department of Chemical Engineering and Biotechnology, University of Cambridge
Philippa Fawcett Drive, Cambridge CB3 0AS

** chc57@cam.ac.uk*

Abstract. The rapid movement of gas-liquid foams through narrow contractions is commercially challenging and technically important, with wide industrial applications, including the flow and moulding of aerated products, e.g. ice cream and shaving foam, foam-sclerotherapy for varicose veins, and oil-well cementing when foam-cement slurries are pumped into narrow annuli. This study investigates the flow of wet foams with a polymeric liquid phase, which has a high viscosity and complex rheology, using a Multi-Pass Rheometer. The in-situ visualization of foam flowing through an orifice, recorded by high-speed camera, reveals rich and complex behaviour and interaction between bubbles. The bubble behaviour in the polymer melt is qualitatively compared with that observed in a highly viscous Newtonian liquid.

Keywords: Polymeric foam, Bubbly liquid, Multi-Pass Rheometer
PACS: 47.50.-d

1. Introduction

Thermoplastic foam is of importance due to its wide applications in various areas: (i) where impact strength is required, (ii) for thermal and electrical insulation, and (iii) for lightweight material-saving structures. The processes for producing polymeric foam range from using polymer with dissolved blowing agents in batch mode processes to using expandable polymer beads containing blowing agents for injection moulding and hot-melt extrusion in continuous foaming processes. The cellular structures of the foams are determined by the effects of polymer properties, the operating conditions such as pressure, temperature, and shear flow, and the foaming mechanisms involving bubble nucleation, bubble growth, and cell coalescence.

The visualization of polymer foaming is useful for studying foaming mechanisms. Many researchers have worked on the in-situ observation of bubble nucleation and growth either in batch foaming or continuous foaming, and directly observe the foaming process during injection moulding or extrusion[1-7]. Experiments have also been conducted to study bubble nucleation in a shear flow field, revealing several kinds of nucleation mechanisms[8-10].

The Multi-Pass Rheometer (MPR) is a twin piston rheometer invented in the early 1990s by Professor Malcolm Mackley at the University of Cambridge. Since then, the MPR has found useful applications in a wide range of areas[11] such as (i) using the MPR as a capillary rheometer for measuring rheological properties of Newtonian and Non-Newtonian liquids, (ii) studies of multiphase fluids, (iii) flow induced birefringence processing, (iv) flow induced crystallisation, (v) polymer melt instability, and (vi) polymer foaming. These studies demonstrated the flexibility of the MPR as a research tool which can be modified for new experiments. The MPR has also been used for studying bubble nucleation and growth in polystyrene melt containing pentane gas[12]. In this paper the MPR has been used to study the flow of highly viscous polymeric foam and to make observation of bubble behaviours as the foam passes through a narrow orifice.

2. Experimental apparatus and procedures

The experiments were performed by using a Multi-Pass Rheometer equipped with an optical module, where a flow chamber is formed by two parallel quartz windows with stainless inserts between the windows. By changing the shape of the inserts, a flow passage with a chosen geometric pattern is obtained; in this work an orifice plate and a contraction-expansion channel were used. Both temperature and pressure were measured by a pair of pressure transducers each with an integrated thermocouple, installed on both ends of the chamber. A separate thermocouple was also placed at the centre of the flow chamber.

The experimental setup is shown in figure 1. A high speed CMOS camera (Balser acA1300-200uc) with LED light source (Thorlabs MCWHLP1) backlighting was used to obtain the bubble images. The white box shown in figure 1 indicates the field of view where the sequential images were recorded. The blue area represents the twin pistons that can generate fluid upflow or downflow through the flow passage; the pink area represents the loaded test liquid. The test liquids were polybutene oil (Brookfield viscosity standard liquid B73000, 73.0 Pa s at 25 °C) and expandable polystyrene (INEOS Styrenics EPS-FR), e.g. polystyrene beads containing pentane. A rotational rheometer (TA instruments ARES), equipped with 20.0 mm diameter parallel plates, was used to measure the apparent viscosities of both liquids; results are shown in figure 2. The expandable polystyrene beads were

degassed by first being loaded into a mould and pressed to a round disc by means of a heated press; some of the gas is released, but some remains in the disc as bubbles. By repeating the same process several times to release the gas, a pentane-free polystyrene disc can be obtained for testing the apparent viscosity of polystyrene melt. The flow curve shown in figure 2 demonstrates the polybutene has a constant apparent viscosity of 67 Pa s, showing that it is a Newtonian liquid. The deviation from the reported 73 Pa s is probably due to temperature effects. The polystyrene melt is shear-thinning, with a zero-shear rate viscosity of about 1250 Pa s

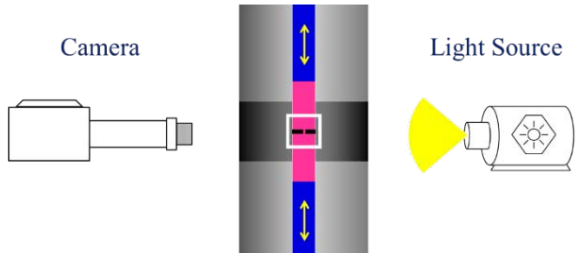

Figure 1. Schematic Diagram of Experiment

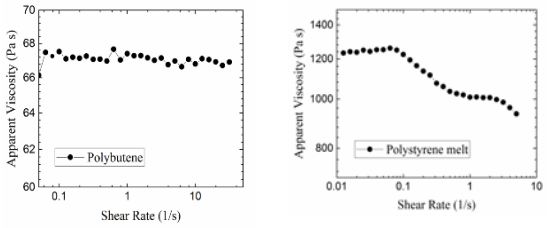

Figure 2. Plots of apparent viscosity as a function of shear rate

The steps of the experimental procedure are as follows:

(i) Assembling the flow chamber by selecting different quartz windows and stainless inserts to obtain the desired geometry of flow passage.

(ii) Loading and preparing the test materials.

The polybutene oil is first premixed with air bubbles which were entrained by hand stirring using a spatula; the bubbly liquid is then injected into the flow chamber using a syringe. Due to the high viscosity of the continuous phase, bubbles are stably suspended within the oil during the experiment; the effects of buoyancy and Ostwald ripening are observed to be relatively slow, hence the position and size distribution of bubbles change negligibly during an experiment.

A different loading protocol is required for bubbly polystyrene melt[12]. The beads, each bead containing dissolved gas, are first loaded into the flow chamber at room temperature and then heated to around 80 °C where they soften without gas release. Then, the beads are further compacted by hand to leave space for additional beads to be added. This compaction and addition process is repeated several times. Finally, the flow chamber is sealed with the upper piston, and the temperature increased to over 110 °C, giving rising to bubble formation, resulting in even bubble distribution within the flow chamber.

A typical transformation of the polystyrene beads containing pentane from solid through to bubbly liquid is shown in figure 3. Initially, the beads appear as dark round spheres, each bead identifiable at room temperature in photo A, loaded into a contracting-expanding flow geometry; then the beads are heated through photos (B), (C) and (D) where they swell as they reach 110 °C until finally forming a bubbly liquid, pentane bubbles in polystyrene liquid, at 160 °C, see photo (E). Increasing the pressure of the melt causes the bubbles to dissolve, so the volume fraction of bubbles diminishes, see photos F, G, and H. Finally, a single phase polymer melt is achieved at photo I.

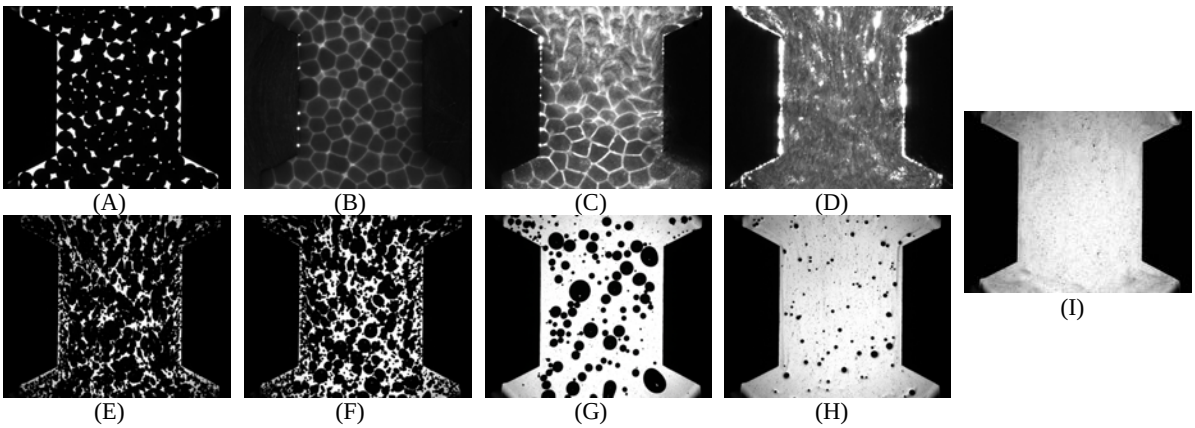

Figure 3. Sequential images illustrating the transformations of the beads from solid through to bubbly liquid.

(iii)Performing experiments.

The upper and lower pistons can be controlled, either individually or together, to generate desired pressure and flow rate within the chamber. Piston velocities ranging from 0.01 up to 10.0 mm/s were used. During a given experiment, images of the bubble motion were recorded using the high speed camera and the differential pressure across the flow geometry was measured.

3. Results and Discussion

Experiments were carried out to visualize the bubbly polymer melt flow. The width of the flow chamber was chosen as 10.0 mm; from this chamber, the flow channel abruptly reduced to a 1.4 mm orifice opening with a length of 1.5 mm. The depth, normal to the flow, was 1.0 mm to reduce overlapping of the bubbles. A typical flow of expandable polystyrene is shown in figure 4; the bubbly polymer melt flowing downward through an orifice and at rest are shown in the left and right photographs, respectively. In these images, bubbles appear as black shadows. The bubbles upstream of the orifice were elongated along the flow direction towards the orifice; whereas downstream the bubbles tended to coalesce into bigger bubbles, giving big dark cavities; these bubbles were stretched perpendicular to the flow direction outward from the orifice. When the flow stopped, all the deformed bubbles gradually returned to spherical shape due to a balance between the viscous and surface tension forces.

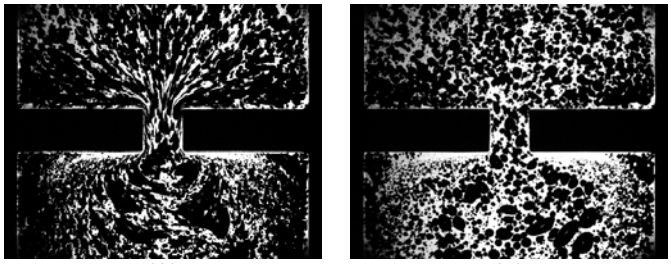

(A) (B)

Figure 4. Typical flow of polymeric foam, bubbly polystyrene melt (A) flowing downwards through an orifice and (B) at rest.

In a system of reduced bubble density, the behaviour of individual bubbles and the interaction between bubbles can be observed more clearly. By carefully manipulating the pressure within the flow chamber, a desired volume fraction of pentane gas in the polystyrene melt can be obtained. Upflow of bubbly polystyrene melt through an orifice, with low bubble volume fraction, is shown in figure 5. The polydisperse pentane bubbles were sparsely and randomly distributed within the flow chamber. In the flowing polymeric melt, the initially spherical bubbles were deformed and elongated as they moved towards the orifice; significant coalescence of the bubbles occurred near the orifice and downstream of the orifice. The dynamics of bubble deformation upstream of the orifice is similar to that observed in a previous study[10]. At a time of 6.25 sec, bigger bubbles with distorted boundaries were observed downstream; here the bubbles are stretched laterally like those observed in dense polymer foam systems. From 12.5 sec, after the start of the experiment, the liquid motion slowed and came to a full stop at 43.25 sec; all the deformed bubbles subsequently relaxed back to a spherical shape.

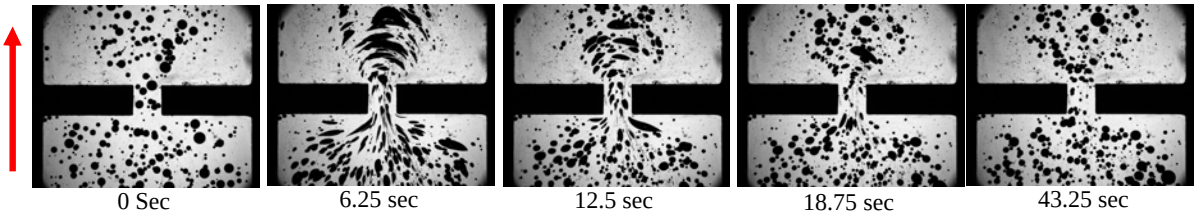

0 Sec 6.25 sec 12.5 sec 18.75 sec 43.25 sec

Figure 5. Pentane gas bubbles in polystyrene melt, non-Newtonian, flowing upward through orifice. Motion slows from 12.5 Sec and stops at 43.25 Sec.

In order to understand the behaviour of the bubbles in non-Newtonian liquid, it is helpful to examine the dynamic behaviour of bubbles in a Newtonian liquid for comparison. Air bubbles in polybutene oil, with a bubble volume fraction similar to that used in the non-Newtonian liquid, are shown flowing through the orifice in figure 6. The bubbly liquid started from rest; the bubbles were deformed and elongated as they approached the orifice as observed in the non-Newtonian liquid. The motion slowed down from 10.0 sec and stopped at 17.5 sec where the spherical shape of bubbles is shown in figure 6. However, coalescence of bubbles was not observed, even for the bigger bubbles; in Figure 6 at 5.0 sec two larger bubbles are seen without coalescence. Bubble coalescence appears to be suppressed in this viscous Newtonian liquid. The bigger bubbles in the Newtonian liquid flowing through the orifice were usually stretched, downstream, into a smooth crescent-shaped bubble with very sharp tips. This is different from the distorted bubble shapes observed under similar conditions in non-Newtonian liquid. The formation of the crescent bubble shape is thought to be due to the radial flow of liquid so that the front of the bubble moves more slowly than the back. The sharp tips of each bubble is preserved from breakup due to the surface tension force being less than viscous force. A separate paper is currently in preparation to discuss these crescent-shaped bubbles in more detail.

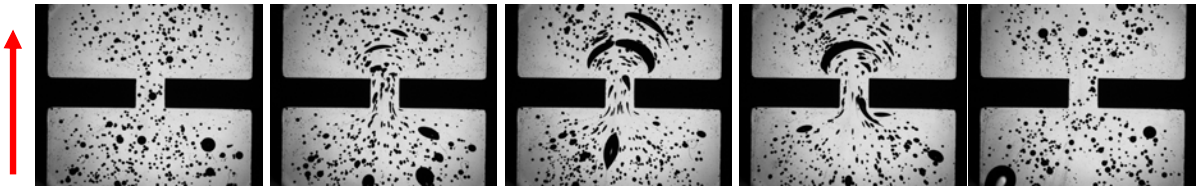

Figure 6. Air bubbles in Polybutene liquid (Newtonian liquid) flowing through Orifice. Motion slows after 10.0 Sec, and stops before 17.5 Sec.

By further increasing the pressure of the fluid, most of the bubbles dissolved, leaving a single bubble or a few bubbles in the polymer melt. This greatly facilitated the study of bubble dynamics in non-Newtonian liquid. Figure 7 shows breakup and coalescence of bubbles in polystyrene melt during the upflow through the orifice, which are not observed in the Newtonian case. Initially, four large spherical bubbles moved from the stationary position; the bubbles were stretched and distorted after passing through the orifice, at the time 1.5 sec. The bubbles were each split up into a major bubble and a satellite bubble due to bubble distortion under the radial flow. Subsequently, there is coalescence of those major bubbles at 2.0 sec. At 2.5 sec, a big bubble is seen flowing towards the orifice, bubble breakup was again observed, giving major and satellite bubbles at 3.5 sec. From 7.0 sec, the flow slowed and the bubbles stopped at 15.0 sec, restoring to spherical shape.

This case shows flow induced bubble breakup and coalescence in non-Newtonian liquid. The mechanism of bubble coalescence, observed in figure 7, can be explained from previous studies on the coalescence between bubbles rising under buoyancy in non-Newtonian liquids[13, 14]. The memory effect of the residual stress in a shear thinning viscoelastic liquid holds for a certain time in the wake of the leading bubble, causing the local viscosity to decrease, which induces acceleration of the following bubble. After coalescence, the resultant bigger bubble will shear the liquid more strongly, accelerating the following bubbles; thus, there is a dynamical competition between the creation and relaxation of stresses due to the consecutive passage of bubbles. When the bubble density is further increased to a certain threshold, the interaction between bubbles is no longer regularly periodic; chaotic coalescence dominates [14, 15].

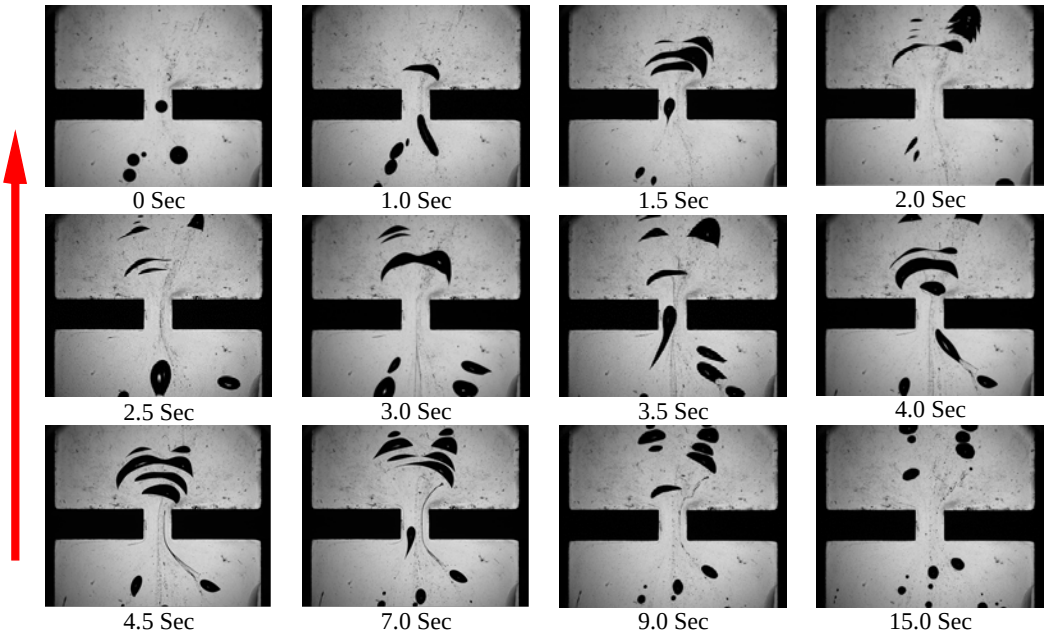

Figure 7. Bubble coalescence and breakup in polystyrene melt, non-Newtonian. Steady upward flow, starting from stationary, at 0 Sec. From 7.0 sec, the flow slows and stops at 15.0 sec.

In figure 8, a 45° contraction-expansion channel with both ends of 10.0 mm width reducing down to a flow chamber with both 6.0 mm in width and length was used to demonstrate this flow-induced coalescence in the polystyrene melt. The channel depth was 1.0 mm, normal to the flow direction. The bubbly polystyrene melt was cyclically moved up and down with a 3.0 sec stop at the end of each moving. In the first downflow, row A in Figure 8, initially spherical bubbles starting from stationary were deformed; significant coalescence of bubbles greatly reduced the bubble number density in the channel. After a 3.0 sec stop, the flow was reversed, row B in figure 8. A large gas cavity and fewer large bubbles passing through the channel were observed. In the subsequent flow cycles, C and D, the large gas cavity became bigger with fewer large bubbles left in the channel.

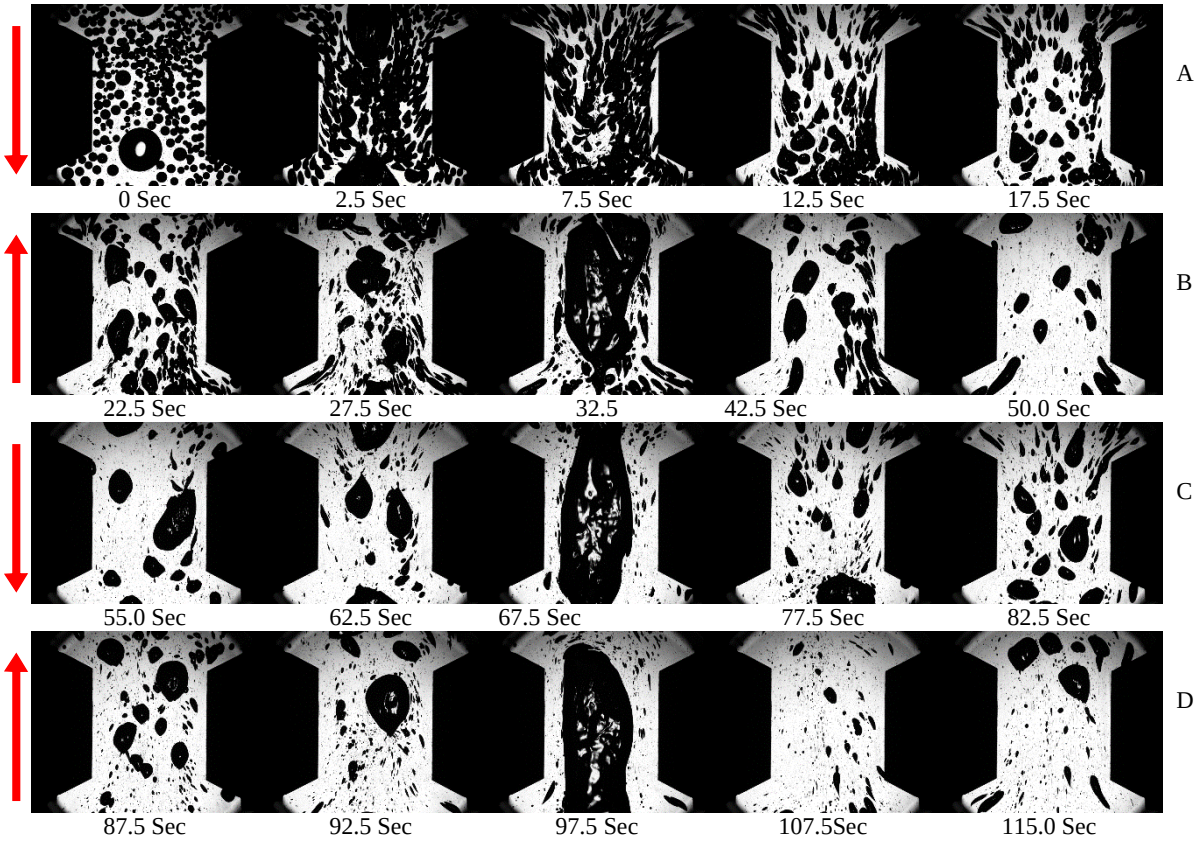

Figure 8. Pentane bubbles in polystyrene melt (Non-Newtonian) flowing cyclically through 45 degree contraction-expansion channel. The arrows denote the upflow or downflow.

Conclusions

Experiments used a Multi-pass rheometer to study the flow of a bubbly polystyrene melt flowing through an orifice or a 45° contraction-expansion channel. By controlling the pressure within the flow chamber, a system of reduced bubble density can be obtained to study the dynamics of single bubble or the interaction between bubbles in polymer melt. The dynamics of bubbles in polystyrene melt, a non-Newtonian liquid, is qualitatively compared with that observed in polybutene oil, a Newtonian liquid, showing great differences of bubble deformation, instability in bubble pinch-off, and flow-induced coalescence, especially downstream of the orifice.

Acknowledgements

The authors thank for the financial support of EPSRC grant, EP/N00230X/1.

References

1. K. Taki, T. Nakayama, T. Yatsuzuka and M. Ohshima, *Journal of Cellular Plastics*, 2003, **39**, 155-169.
2. C. D. Han and C. A. Villamizar, *Polymer Engineering & Science*, 1978, **18**, 687-698.
3. C. A. Villamizar and C. D. Han, *Polymer Engineering & Science*, 1978, **18**, 699-710.
4. A. Ahmadzai, A. H. Behravesh, M. T. Sarabi and P. Shahi, *Journal of Cellular Plastics*, 2014, **50**, 279-300.
5. V. Shaayegan, L. H. Mark, A. Tabatabaei and C. B. Park, *Express Polymer Letters*, 2016, **10**, 462-469.
6. Q. P. Guo, J. Wang, C. B. Park and M. Ohshima, *Industrial & Engineering Chemistry Research*, 2006, **45**, 6153-6161.
7. C. D. Han and H. J. Yoo, *Polymer Engineering and Science*, 1981, **21**, 518-533.
8. J. H. Han and C. D. Han, *Polymer Engineering & Science*, 1988, **28**, 1616-1627.
9. A. Wong and C. B. Park, *Polymer Testing*, 2012, **31**, 417-424.
10. H. J. Yoo and C. D. Han, *Polymer Engineering & Science*, 1981, **21**, 69-75.
11. M. R. Mackley and D. G. Hassell, *Journal of Non-Newtonian Fluid Mechanics*, 2011, **166**, 421-456.
12. T. R. Tuladhar and M. R. Mackley, *Chemical Engineering Science*, 2004, **59**, 5997-6014.
13. H. A. Z. Li, *Chemical Engineering Science*, 1999, **54**, 2247-2254.
14. H. Z. Li, X. Frank, D. Funfschilling and Y. Mouline, *Chemical Engineering Science*, 2001, **56**, 6419-6425.
15. H. Z. Li, Y. Mouline, L. Choplin and N. Midoux, *International Journal of Multiphase Flow*, 1997, **23**, 713-723.